

RFBNet: Deep Multimodal Networks with Residual Fusion Blocks for RGB-D Semantic Segmentation

Liuyuan Deng, Ming Yang, Tianyi Li, Yuesheng He, and Chunxiang Wang

Abstract—Signals from RGB and depth data carry complementary information about the scene. Conventional RGB-D semantic segmentation methods adopt two-stream fusion structure which uses two modality-specific encoders to extract features from the RGB and depth data. There is currently no explicit mechanism to model the interdependencies between the encoders. This letter proposes a novel bottom-up interactive fusion structure which introduces an interaction stream to bridge the modality-specific encoders. The interaction stream progressively aggregates modality-specific features from the encoders and computes complementary features for the encoders. To instantiate this structure, the letter proposes a residual fusion block (RFB) to formulate the interdependencies of the encoders. The RFB consists of two residual units and one fusion unit with gate mechanism. It learns complementary features for the modality-specific encoders and extracts modality-specific features as well as cross-modal features. Based on the RFB, the letter presents the deep multimodal networks for RGB-D semantic segmentation called RFBNet. The experiments conducted on two datasets demonstrate the effectiveness of modeling the interdependencies and that the RFBNet outperforms state-of-the-art methods.

Index Terms—RGB-D data, semantic segmentation, convolutional neural network, multimodal fusion.

I. INTRODUCTION

Semantic segmentation, which is also termed as image parsing, is the task of assigning each pixel with a semantic label from a given class set [1], [2]. In recent years, with the success of the convolutional neural networks in vision recognition [3], [4], most state-of-the-art semantic segmentation methods employ fully convolutional neural networks usually with an encoder-decoder architecture using visual signals (i.e., RGB images) [5]–[8]. As depth signals provide complementary information to the visual signals, increasing research exploits deep multimodal networks to fuse the two modalities [9]–[14]. This letter explores the fusion structures of multimodal networks for RGB-D semantic segmentation.

The fusion approaches can be categorized into early, late, and hierarchical fusion [14]. Early fusion approaches (see Fig. 1(a)) simply feed the concatenated RGB and depth channels into a conventional unimodal network [9]. Such methods may not fully exploit the complementary nature of the modalities [15]. Many works turn to the two-stream fusion architecture which processes each modality by a separated

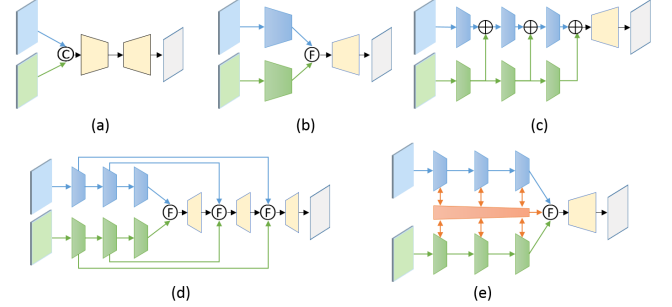


Fig. 1. Fusion structures for RGB-D semantic segmentation. The blue color and green color indicate RGB stream and depth stream, respectively. The trapezoids indicate encoder layers and decoder layers. \odot and \oplus denote the concatenation and summation operations; \oplus denotes a combination method. (a) Early fusion (b) Late fusion (c) Fusing multi-level depth features into RGB stream. (d) Top-down multi-level fusion. (e) The proposed bottom-up interactive fusion.

and identical encoder and fuses modality-specific features in a single decoder [10]–[14]. The late fusion approaches [10], [11] (see Fig. 1(b)) combine the modality-specific features at the end of the two independent encoders with a combination method, e.g., concatenation and element-wise summation. Instead of fusing at early or late stages, hierarchical fusion involves fusing the features at multiple levels. FuseNet [12] fused multi-level depth features into the RGB encoder in the bottom-up path (see Fig. 1(c)). SSMA [14] and RDFNet [13] fused multi-level features in the top-down path (see Fig. 1(d)). Although these approaches have achieved encouraging results, they do not fully exploit the interdependencies of the modality-specific encoders. We argue that the two encoders benefit from interacting and informing each other.

In this letter, we propose a bottom-up interactive fusion structure which bridges the modality-specific streams, i.e., RGB stream and depth stream, with an interaction stream. The structure should address two aspects. First, it should progressively aggregate the information from the modality-specific streams to the interaction stream and extract the cross-modal features. Second, it should compute complementary features and feed them to the modality-specific streams without destroying the encoders' ability to extract modality-specific features. The structure is illustrated in Fig.1(e).

To instantiate this structure, we propose a residual fusion block (RFB) to formulate the interdependencies of the two encoders. The RFB consists of two modality-specific residual units (RUs) and one gated fusion unit (GFU). The GFU adaptively aggregates features from the RUs and generates complementary features for the RUs. The RFB formulates the

This work is supported by the National Natural Science Foundation of China (U1764264/61873165), Shanghai Automotive Industry Science and Technology Development Foundation (1733/1807), International Chair on automated driving of ground vehicle. Ming Yang is the corresponding author.

The authors are with Department of Automation, Shanghai Jiao Tong University, Key Laboratory of System Control and Information Processing, Ministry of Education of China, Shanghai, 200240, China (phone: +86-21-34204553; e-mail: MingYang@sjtu.edu.cn).

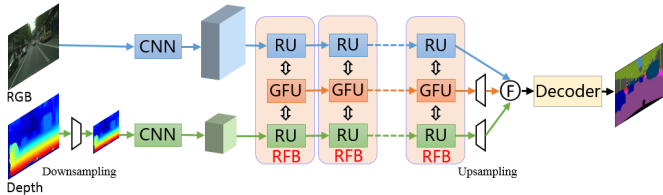


Fig. 2. The architecture of the RFBNet. The three bottom-up streams are highlighted by different colors: RGB stream (blue), depth stream (green), and interaction stream (orange). The RFB manages the interaction of the three streams. \oplus denotes the combination method.

complementary feature learning as residual learning, and it can extract modality-specific and cross-modal features. With the RFBs, the modality-specific encoders can interact with each other. We build the deep multimodal networks for RGB-D semantic segmentation based on the RFB, which is called RFBNet. We verify the RFBNet on indoor and outdoor datasets including ScanNet [16] and Cityscapes [17]. The RFBNet constantly outperforms the baselines. Particularly, the model achieves 59.2% mIoU on ScanNet test set.

II. BOTTOM-UP INTERACTIVE FUSION WITH RESIDUAL FUSION BLOCKS

A. Architecture

The architecture of the proposed RFBNet is illustrated in Fig. 2. Besides the RGB stream and depth stream, the architecture introduces an additional interaction stream. The three streams are merged by a combination method which can be concatenation, summation, SSMA block [14], etc. Finally, a decoder is appended to compute the predictions. The RFBs are employed at high layers to manage the interaction of the three streams. Specifically, the RFBs are employed at layers after three downsampling operations when the spatial size of the feature map is one eighth that of the input data. Moreover, the spatial size of the interaction stream is the same as that of the depth stream, and the channel dimension is half of that of the depth stream.

The architectures with two encoders suffer from large computational and memory consumption. RGB data contains rich appearance and textural details to depict the objects, while depth data contains relatively sparse geometric information to depict the shape of objects. We ease the consumption by shrinking the spatial size of the depth stream. We shrink the depth data by a factor of 2 before inputting into the net, which reduces roughly three-quarters of computation and memory consumption for the depth stream. The depth stream and the interaction stream are upsampled to the same spatial size as the RGB stream before combining.

B. Residual Fusion Block

The RFB is the basic module to achieve the idea of bottom-up interactive fusion. The RFB consists of two modality-specific residual units (RUs) and one gated fusion unit (GFU). The RU, as the basic unit of ResNet [4], is widely used in unimodal networks to learn unimodal features. The RFB learns the modality-specific features based on the RU. We design the

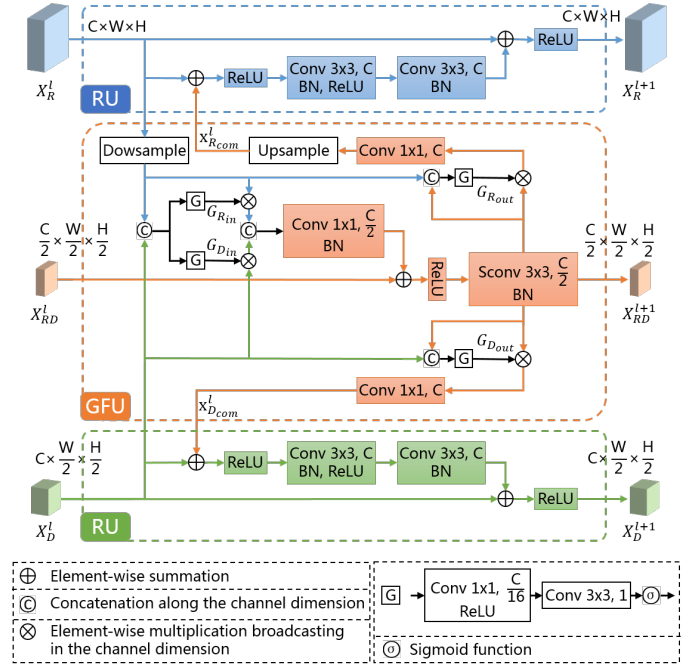


Fig. 3. The framework of the residual fusion block. The block consists of two RUs and one GFU. It manages three streams: RGB, depth, and interaction streams, and formulates the interdependencies of the modality-specific streams.

GFU to aggregate features from the modality-specific RUs and compute complementary features for the RUs. The framework of the RFB is illustrated in Fig. 3.

Given the input RGB, depth, and cross-modal features $x_R^l \in \mathbb{R}^{C \times H \times W}$, $x_D^l \in \mathbb{R}^{C \times \frac{H}{2} \times \frac{W}{2}}$, $x_{RD}^l \in \mathbb{R}^{\frac{C}{2} \times \frac{H}{2} \times \frac{W}{2}}$ and the output features $x_R^{l+1} \in \mathbb{R}^{C \times H \times W}$, $x_D^{l+1} \in \mathbb{R}^{C \times \frac{H}{2} \times \frac{W}{2}}$, $x_{RD}^{l+1} \in \mathbb{R}^{\frac{C}{2} \times \frac{H}{2} \times \frac{W}{2}}$, the RFB is formulated as:

$$x_{R_{com}}^l, x_{RD}^{l+1}, x_{D_{com}}^l = \mathcal{G}(x_R^l, x_{RD}^l, x_D^l) \quad (1)$$

$$x_R^{l+1} = x_R^l + \mathcal{F}_R(x_R^l + x_{R_{com}}^l, \mathcal{W}_R^l) \quad (2)$$

$$x_D^{l+1} = x_D^l + \mathcal{F}_D(x_D^l + x_{D_{com}}^l, \mathcal{W}_D^l) \quad (3)$$

where $x_{R_{com}}^l$ and $x_{D_{com}}^l$ are the complementary features computed by the GFU denoted as \mathcal{G} ; \mathcal{F}_R and \mathcal{F}_D denotes the residual functions of the modality-specific RUs; \mathcal{W}_R^l and \mathcal{W}_D^l are parameters of the RUs.

From the (2) and (3), we can see the modality-specific RUs have the same parameter form with the standard RU [4]. The difference is that we add complementary features to the input of the RUs.

The RFB formulates the complementary feature learning as residual learning. The GFU acts as a residual function with respect to an identity mapping as illustrated in Fig. 4(b). Note that we add the complementary features $x_{R_{com}}^l$ and $x_{D_{com}}^l$ to the inputs of the modality-specific residual functions (denoted as Point ‘‘R’’) instead of the trunks of the unimodal streams (denoted as Point ‘‘T’’). The different adding points imply different identity mappings as illustrated in Fig. 4. The complementary feature directly impacts the modality-specific stream when adding to Point ‘‘T’’ (see Fig. 4(a)), while it

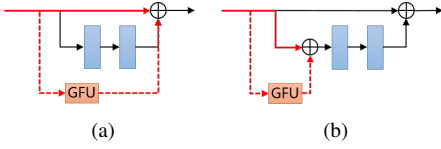


Fig. 4. The flows of the residual and identity mappings when adding complementary features at different points. The GFU acts as a residual function with respect to an identity mapping. The red solid arrow indicates the information flow of identity mapping, while the red dashed arrow indicates the information flow of residual mapping. (a) Adding to the trunk (Point “T”). (b) Adding to the input of the residual function of the RU (Point “R”).

directly impacts the residual function of the modality-specific RU when adding to Point “R” (see Fig. 4(b)).

Redundancy, noise, and complementary information exist among different modalities. The GFU explores the underlying complementary relationships in a soft-attention manner via the gate mechanism. Gates are commonly used to regulate the flow of the information [11], [18], [19]. For example, Hochreiter et al. [18] used four gates to control the information propagate in and out of the memory cell and Cheng et al. [11] used weighted gates to combine features from different modalities automatically.

The GFU contains two input gates and two output gates. The input gates $G_{R_{in}}, G_{D_{in}} \in \mathbb{R}^{1 \times \frac{H}{2} \times \frac{W}{2}}$ are used to control the unimodal features to flow into the interaction stream, and the output gates $G_{R_{out}}, G_{D_{out}} \in \mathbb{R}^{1 \times \frac{H}{2} \times \frac{W}{2}}$ are used to regulate the complementary features. The gates are learned by the same network $G(\cdot)$ as shown in the bottom of Fig. 3. $G(\cdot)$ consists of two convolutional layers with a ReLU layer in between, and a Sigmoid function $\sigma(\cdot)$ to squash values to $[0, 1]$ range. Note that we share the first convolutional layer for input gates to reduce the computational cost.

The useful information regulated by the input gates is concatenated together, following a 1×1 convolutional layer before adding to x_{RD}^l (x_{RD}^l is zero for the first RFB). Then we adopt a light-weight depthwise separable convolution (denoted as “Sconv” in Fig. 3) [20] to process the cross-modal features in the interaction stream. Finally, the GFU compute the complementary features for the modality-specific RUs regulated by the two output gates $G_{R_{out}}$ and $G_{D_{out}}$.

C. Incorporating with Top-Down Multi-Level Fusion

The proposed bottom-up interactive fusion structure models the interdependencies for the modality-specific encoders. It is orthogonal to the top-down multi-level fusion structure which fuses the encoders features in the top-down path at the decoder stage. The two structures can incorporate into a united network. In the experiments, we employ our approach in the SSMA [14] which adopts the top-down multi-level fusion.

III. EXPERIMENTAL RESULTS

A. Setup

Datasets. ScanNet is a large-scale indoor scene understanding benchmark. It contains 19,466 samples for training, 5,436 for validation, and 2,537 for testing. The RGB images are captured at a resolution of 1296×968 and depth at 640×480 . Cityscapes is an outdoor RGB-D dataset for urban

scene understanding. It contains totally 5,000 finely annotated samples with a resolution of 2048×1024 , of which 2,975 for training, 500 for validation, and 1,525 for testing..

Backbones. We adopt two unimodal backbones, i.e., AdapNet++ [14] and ERFNet [6]. AdapNet++ is based on the ResNet-50 model with full pre-activation bottleneck residual units, while ERFNet is a real-time semantic segmentation model based on non-bottleneck factorized residual units. We use the encoder model of the ERFNet (denoted as ERFNetenc) for fast testing and ablation study.

Criteria. We quantify the performance according to the PASCAL VOC intersection-over-union metric (IoU) [21].

B. Implementation Details

We first built up two-stream fusion networks with the unimodal backbones. We adopt SSMA [14], a state-of-the-art method, as the base framework which uses SSMA blocks to combine the two modality-specific streams. The $SSMA_{(AdapNet++)}$ is the same as SSMA model proposed in [10]. For the $SSMA_{(ERFNetEnc)}$, we use the ERFNetenc to extract two modality-specific features, combine the features with the SSMA block, and use a 1×1 convolutional layer and a bi-linear interpolation upsampling layer by a factor of 8 to get the final predictions. To employ our approach, we just replace the corresponding paired RUs with the RFBs for $RFBNet_{(AdapNet++)}$ and $RFBNet_{(ERFNetenc)}$. When employing the RFB for the bottleneck residual units, we feed the features output by the first 1×1 layers of the bottleneck RUs to GFU, and add the complementary features to the inputs of the 3×3 layers of the RUs.

The models were implemented using the Tensorflow 1.3.0. Adam is used for optimization, and “poly” learning rate scheduling policy is adopted to adjust the learning rate. The weight decay is set to $5e^{-4}$ for the AdapNet++ based models and $1e^{-4}$ for the ERFNetenc based models. The images are resized to a smaller scale for training so that the models can be trained on our 1080Ti GPU. For ScanNet, the images are resized to 640×480 ; For Cityscapes, the images are resized to 1024×512 . We resize the predictions to the full resolution when benchmarking. When training on Cityscapes, we employ a crop of 768×384 . We perform depth completion [22] for the depth images and employ the three-channel HHA encoding [23] for the depth data.

We first train the unimodal models, then use the trained weights to initialize the encoders of the multimodal models. For the AdapNet++ based models, we follow the training procedure of [14]. We set a mini-batch of 7 for unimodal models, 6 for multimodal models, and 12 for finetuning. For the ERFNetenc based models, we use an initial learning rate of $5e^{-4}$. We train 100K iterations with a mini-batch of 12 for the unimodal models, and 25K iterations with a mini-batch of 9 for the multimodal models. We employed extensive data augmentations, including flipping, scaling, rotation, cropping, color jittering, and Gaussian noise.

C. Results and Analysis

Benchmarking. We report the performance benchmarking results on ScanNet and Cityscapes in Table I and Table II.

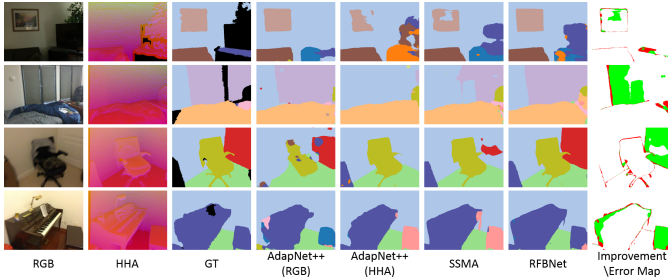


Fig. 5. Qualitative results of RFBNet compared with baseline unimodal and multimodal methods on ScanNet dataset. The last column shows the improvement/error map which denotes the misclassified pixels in red and the pixels that are misclassified by SSMA but correctly predicted by RFBNet in green.

Note that the test images of the two datasets are not publicly released, and they are used by the evaluation server for benchmarking. From the tables, we can see that the multimodal models have better performance than the unimodal models as expected. In Table I, we compare against the top performing models on ScanNet. The proposed RFBNet outperforms other methods on the leaderboard, e.g., SSMA [14], FuseNet [12] and 3DMV [24]. Note that the RFBNet and SSMA adopted the same backbone, i.e., AdapNet++, and the RFBNet achieved 1.5% improvement over SSMA. In Table II, we compare RFBNet with base models of different backbones on Cityscapes, which shows that the proposed RFBNet constantly outperforms SSMA with different backbones. We found that the multimodal models improve less on Cityscapes than on ScanNet. We infer the reason is that the depth values of the outdoor data are much more noisy than those of the indoor data. Some parsing results on ScanNet are shown in Fig. 5.

Ablation Study. We perform the ablation study on the ScanNet validation set with the ERFNetenc backbone. In Table III, we compare the performance of unimodal models and multimodal models and show how the resolution of the depth

TABLE I
EVALUATION RESULTS ON THE SCANNET TEST SET.

Network	Multimodal	mIoU
PSPNet	-	47.5
AdapNet++	-	50.3
3DMV (2d proj)	✓	49.8
FuseNet	✓	52.1
SSMA	✓	57.7
RFBNet	✓	59.2

TABLE II
EVALUATION RESULTS ON THE CITYSCAPES DATASET WITH DIFFERENT BACKBONES (INPUT IMAGE DIM: 1024×512).

Method	Multimodal	mIoU@val	mIoU@test
ERFNetEnc	-	69.5	67.1
SSMA _(ERFNetEnc)	✓	70.8	68.9
RFBNet _(ERFNetEnc)	✓	72.0	69.7
AdapNet++	-	73.4	73.2
SSMA _(AdapNet++)	✓	75.0	74.2
RFBNet _(AdapNet++)	✓	76.2	74.8

TABLE III
RESULTS OF ERFNETENC BASED MODELS ON THE SCANNET VALIDATION SET WITH DIFFERENT RESOLUTIONS OF DEPTH DATA.

Method	Input data	Shrink depth	mIoU
ERFNetEnc	RGB	-	51.7
ERFNetEnc	Depth	-	56.7
SSMA	Multimodal	×	61.6
SSMA	Multimodal	✓	61.1
RFBNet	Multimodal	×	62.2
RFBNet	Multimodal	✓	62.6

TABLE IV
PERFORMANCE OF RFBNET_(ERFNETENC) ON SCANNET VALIDATION SET FOR DIFFERENT SETTINGS OF THE RESIDUAL FUSION BLOCK.

G	T	R	mIoU
			61.3
✓			61.7
✓	✓		62.0
✓		✓	62.6

data impact the performance. From Table III, we can see the multimodal models show a large improvement over unimodal models by more than 4%. When shrinking the depth input, the SSMA shows performance decrease by 0.5%. We analyze that shrinking the depth can relatively increase the receptive field of depth encoders, which is beneficial for capturing broader context information, but it may lose some geometric details and reduce the spatial representation accuracy. Thus, the performance of SSMA which adopts independent encoders decreases. As the RFBNet bridges the encoders with an interaction stream, both of the unimodal encoders benefit from broader context information. Although losing some geometric details, RFBNet still shows performance improvement by 0.4%.

We show how the gates and complementary adding points of the RFB impact the performance in Table IV. “G” means employing gate mechanism to regulate the features. “T” and “R” means the complementary features are added to the trunk and the input of the residual function of RU, respectively. When “T” and “R” are disabled, the interaction stream only aggregates features from unimodal encoders but does not compute complementary features for the encoders. From the table, we can see that the performance improves by 0.4% when employing gates. Moreover, enabling “R” further improves by 0.9% and outperforms enabling “T” by 0.6%, which indicates that it is beneficial for the encoders to interact and inform each other.

IV. CONCLUSION

This letter addresses the RGB-D semantic segmentation by explicitly modeling the interdependencies of the RGB stream and depth stream. We proposed a bottom-up interactive fusion structure to bridge the modality-specific encoders with an interaction stream. Specifically, we proposed the residual fusion block to explicitly formulate the interdependencies of the two encoders. Experiments demonstrate the effectiveness of modeling the interdependencies and that the RFBNet outperforms state-of-the-art methods.

REFERENCES

- [1] G. Zhang and X. Gong, "Nonnegative matrix cofactorization for weakly supervised image parsing," *IEEE Signal Process. Lett.*, vol. 23, no. 11, pp. 1682–1686, 2016.
- [2] S. Wang and Y. Wang, "Weakly supervised semantic segmentation with a multiscale model," *IEEE Signal Process. Lett.*, vol. 22, no. 3, pp. 308–312, 2014.
- [3] O. Russakovsky, J. Deng, H. Su, J. Krause, S. Satheesh, S. Ma, Z. Huang, A. Karpathy, A. Khosla, M. Bernstein *et al.*, "Imagenet large scale visual recognition challenge," *Int. J. Comput. Vis.*, vol. 115, no. 3, pp. 211–252, 2015.
- [4] K. He, X. Zhang, S. Ren, and J. Sun, "Deep residual learning for image recognition," in *IEEE Conf. Comput. Vis. Pattern Recog.*, 2016, pp. 770–778.
- [5] E. Shelhamer, J. Long, and T. Darrell, "Fully convolutional networks for semantic segmentation," *IEEE Trans. Pattern Anal. Mach. Intell.*, vol. 39, no. 4, pp. 640–651, April 2017.
- [6] E. Romera, J. M. Alvarez, L. M. Bergasa, and R. Arroyo, "ERFNet: Efficient Residual Factorized ConvNet for Real-Time Semantic Segmentation," *IEEE Trans. Intell. Transp. Syst.*, 2017.
- [7] L.-C. Chen, Y. Zhu, G. Papandreou, F. Schroff, and H. Adam, "Encoder-decoder with atrous separable convolution for semantic image segmentation," in *Eur. Conf. Comput. Vis.*, 2018, pp. 801–818.
- [8] H. Zhao, J. Shi, X. Qi, X. Wang, and J. Jia, "Pyramid scene parsing network," in *IEEE Conf. Comput. Vis. Pattern Recog.*, July 2017, pp. 6230–6239.
- [9] C. Couprie, C. Farabet, L. Najman, and Y. LeCun, "Indoor semantic segmentation using depth information," *arXiv preprint arXiv:1301.3572*, 2013.
- [10] A. Valada, G. L. Oliveira, T. Brox, and W. Burgard, "Deep multi-spectral semantic scene understanding of forested environments using multimodal fusion," in *Int. Symp. Exp. Robot.* Springer, 2016, pp. 465–477.
- [11] Y. Cheng, R. Cai, Z. Li, X. Zhao, and K. Huang, "Locality-sensitive deconvolution networks with gated fusion for rgb-d indoor semantic segmentation," in *IEEE Conf. Comput. Vis. Pattern Recog.*, 2017, pp. 3029–3037.
- [12] C. Hazirbas, L. Ma, C. Domokos, and D. Cremers, "Fusenet: Incorporating depth into semantic segmentation via fusion-based cnn architecture," in *Asian Conf. Comput. Vis.* Springer, 2016, pp. 213–228.
- [13] S.-J. Park, K.-S. Hong, and S. Lee, "Rdfnet: Rgb-d multi-level residual feature fusion for indoor semantic segmentation," in *IEEE Int. Conf. Comput. Vis.*, 2017, pp. 4980–4989.
- [14] A. Valada, R. Mohan, and W. Burgard, "Self-supervised model adaptation for multimodal semantic segmentation," *arXiv preprint arXiv:1808.03833*, 2018.
- [15] J. Ngiam, A. Khosla, M. Kim, J. Nam, H. Lee, and A. Y. Ng, "Multimodal deep learning," in *Int. Conf. Mach. Learn.*, 2011, pp. 689–696.
- [16] A. Dai, A. X. Chang, M. Savva, M. Halber, T. Funkhouser, and M. Nießner, "Scannet: Richly-annotated 3d reconstructions of indoor scenes," in *IEEE Conf. Comput. Vis. Pattern Recog.*, 2017, pp. 5828–5839.
- [17] M. Cordts, M. Omran, S. Ramos, T. Rehfeld, M. Enzweiler, R. Benenson, U. Franke, S. Roth, and B. Schiele, "The cityscapes dataset for semantic urban scene understanding," in *IEEE Conf. Comput. Vis. Pattern Recog.*, 2016, pp. 3213–3223.
- [18] S. Hochreiter and J. Schmidhuber, "Long short-term memory," *Neural computation*, vol. 9, no. 8, pp. 1735–1780, 1997.
- [19] X. Li, H. Zhao, L. Han, Y. Tong, and K. Yang, "Gff: Gated fully fusion for semantic segmentation," *arXiv preprint arXiv:1904.01803*, 2019.
- [20] A. G. Howard, M. Zhu, B. Chen, D. Kalenichenko, W. Wang, T. Weyand, M. Andreetto, and H. Adam, "Mobilenets: Efficient convolutional neural networks for mobile vision applications," *arXiv preprint arXiv:1704.04861*, 2017.
- [21] M. Everingham, S. A. Eslami, L. Van Gool, C. K. Williams, J. Winn, and A. Zisserman, "The pascal visual object classes challenge: A retrospective," *Int. J. Comput. Vis.*, vol. 111, no. 1, pp. 98–136, 2015.
- [22] J. Ku, A. Harakeh, and S. L. Waslander, "In defense of classical image processing: Fast depth completion on the cpu," in *Conf. Comput. Robot Vis.* IEEE, 2018, pp. 16–22.
- [23] S. Gupta, R. Girshick, P. Arbeláez, and J. Malik, "Learning rich features from rgb-d images for object detection and segmentation," in *Eur. Conf. Comput. Vis.* Springer, 2014, pp. 345–360.
- [24] A. Dai and M. Nießner, "3dmv: Joint 3d-multi-view prediction for 3d semantic scene segmentation," in *Eur. Conf. Comput. Vis.*, 2018, pp. 452–468.